

Towards the Quantitative Prediction of the Phase Behavior of Polymer Solutions by Computer Simulation

Kurt Binder,^{*1} Bortolo Matteo Moggetti,¹ Luis Gonzalez Macdowell,²
Martin Oettel,¹ Wolfgang Paul,¹ Peter Virnau,¹ Leonid Yelash¹

Summary: The phase diagram of polymer solutions (cf. e.g. alkanes dissolved in supercritical carbon dioxide) is complicated, since there are four control parameters (temperature, pressure, monomer volume fraction, chain length of the polymer) and due to the interplay of liquid-vapor transitions and fluid-fluid unmixing. As a result very intricate phase diagram topologies can result. An attempt to develop coarse-grained models that can deal with this task will be described. As usual, the polymers will be modelled as off-lattice bead-spring chains, where several chemical monomers are integrated into one effective bond, torsional degrees of freedom being disregarded. But also a coarse-grained description of the solvent is needed: we show that using a simple point particle with a quadrupole moment and suitable Lennard-Jones interaction yields a very good description of pure carbon dioxide (better than fully atomistic models with potentials from *ab initio* quantum chemistry calculations). The strength of the quadrupole moment is taken from experiment, and the Lennard-Jones parameters are adjusted such that the experimental critical temperature and density is correctly reproduced. This procedure works for other solvents as well, such as benzene. The pure alkane phase diagram is also reproduced by similarly chosen Lennard-Jones (LJ) potentials among the monomers, and the monomer-carbon dioxide LJ parameters are chosen from Lorentz-Berthelot mixing rules. These parameters are then used as input both for Monte Carlo calculations and approximate methods to calculate the equation of state, such as density functional and perturbation theory methods. Apart from the region close to critical points, where mean-field type methods fail, the analytical calculations agree well with the simulations. The solvent model, in which quadrupolar interactions are explicitly considered, is important in order to obtain a fair agreement with mixture experimental results.

Keywords: carbon dioxide; monte carlo simulations; polar fluids

Introduction

Understanding the phase behavior of polymer solutions has been a long-standing challenge.^[1,2] If the solution can be approximated as incompressible, the qualitative behavior can be understood by Flory-Huggins lattice

mean field theory,^[1,2] which predicts that the critical temperature T_c is depressed by a term proportional to $1/\sqrt{n}$ underneath the theta temperature (n being the number of effective segments of the flexible polymer). The monomer volume fraction at the critical point also scales like $1/\sqrt{n}$.

In many cases of interest, however, the solvent is compressible, e.g. in the practically important case of supercritical carbon dioxide.^[3,4] Then, one has four control parameters: temperature T , pressure p , mole fraction of the solute x , and degree of

¹ Institut für Physik, Johannes Gutenberg Universität Mainz, Staudinger Weg 7, 55099 Mainz, Germany
E-mail: kbinder@uni-mainz.de

² Dpto de Química Física, Facultad de Cc. Químicas, Universidad Complutense, 28040 Madrid, Spain

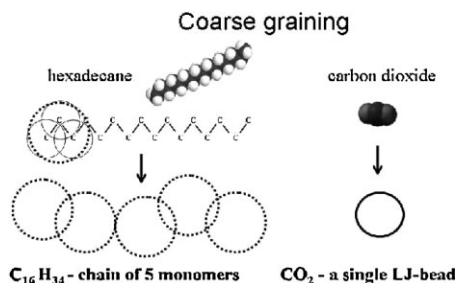
polymerization n of the dissolved polymers. In fact, from the point of view of materials development and processing, it is of practical interest when many control parameters can be used as tools to tailor materials properties. E.g., polystyrene (and other polymers) dissolved in CO_2 can be used to produce polymeric foams, and by suitable choice of p and T , one can vary the cell diameter of these porous materials by two orders of magnitude.^[5]

However, the theoretical understanding of compressible binary fluid mixtures is a difficult problem even for mixtures of small molecules.^[6,7] The simplest case is a “type I”^[6,7] phase diagram: the fluid mixture is miscible for all x , only liquid vapour transitions occur, ending in critical points $T_c^{(1)}$, $T_c^{(2)}$, for the two pure constituents. In the space (T, p, x) , a critical line $T_c(x)$ leads from $T_c^{(1)}$, for $x=0$, to $T_c^{(2)}$, for $x=1$. However, when liquid-liquid immiscibility comes into play, much more complicated phase diagram topologies are possible.^[7] For example, the solution of hexadecane ($\text{C}_{16}\text{H}_{34}$) in CO_2 is believed^[8,9] to belong to “class III” of the Scott-van Konynenburg classification. The line of critical points that starts from the critical point $T_c^{(1)} = T_c(x=0)$ of CO_2 does not go all the way to the critical point $T_c^{(2)} = T_c(x=1)$ of $\text{C}_{16}\text{H}_{34}$, but rather it ends in a “critical end point” at the triple line describing three-phase equilibrium between two liquid-like phases and one vapor-like phase. The line of critical points $T_c(x)$ near $x=1$, on the other hand, first leads to a pressure maximum as $T_c(x)$ decreases with decreasing x , and then reaches a pressure minimum, before it bends over to reach very large pressures. It should be stressed that even for this (chemically very simple!) model system, the detailed phase behavior is not yet known experimentally, and dealing with such problems theoretically, obviously, would be desirable but difficult. In fact, if the vision to reliably predict such phase diagrams from first principles via atomistic simulations, using intermolecular potentials^[10] derived from quantum chemistry, could be turned into reality, many indus-

tries would profit, and clearly this would also be a major success of fundamental statistical mechanics. Unfortunately, as we shall see, we are still very far from this goal. In Section II, we shall now describe the state of the art of modelling the phase behavior of simple one-component fluids. Section III then discusses the issue how well the developed simple models of fluids together with the Lorentz-Berthelot mixing rule^[6,10] does account for the phase behavior of mixtures. A crucial input of this analysis is the fact that modern methods of Monte Carlo simulation together with finite size scaling analyses can yield a numerically essentially exact description of the phase behavior of given model systems: in cases where this description of the pure constituents of a binary mixture is in almost perfect agreement with the corresponding experimental data,^[11] a meaningful test of the mixing rule and its accuracy becomes possible. If the latter is tested by approximate analytic equations of state (EOS), with their parameters for the pure systems fitted to the data, the inaccuracies involved in the statistical mechanical approximate derivations of these EOS necessarily lead to systematic errors in the interaction parameters extracted from such fits. Using such interaction parameters for the description of mixtures, it is clearly impossible to unambiguously disentangle errors due to the mixing rule from errors due to such inappropriate choices of interaction parameters. The last paragraph of section III then summarizes the conclusions of our analysis, which is based on an analysis of mixtures of CO_2 with various alkanes, and other small molecule mixtures.

Coarse-Grained Models for Carbon Dioxide and Other Small Molecules

Due to the complexity of phase diagrams such as that of the $\text{CO}_2 + \text{C}_{16}\text{H}_{34}$ system, it would be a waste of effort, and simply a mistake, to try a very detailed chemically accurate atomistic model of such a system; rather than using all-atom models, we aim

**Figure 1.**

(Color online) Illustration of the coarse-graining procedure: in the case of hexadecane, three successive C–C bonds are integrated into one bead (dotted circle). The oligomer, containing 50 atoms (or 16 “united atoms”, CH₃ or CH₂, respectively) is thus reduced to a chain of only 5 effective beads. Neighboring beads along a chain interact with a combination of Lennard-Jones (LJ) and finitely extensible nonlinear elastic (FENE) potentials. Non-bonded beads only interact with a simple LJ potential. Carbon dioxide is represented by a point particle, but carries a quadrupole moment.

at a coarse-grained description (Figure 1). Thus, the hydrogens of the alkane chains are never explicitly considered, and also CH₂ or CH₃ groups are not treated individually, but three subsequent C–C bonds are lumped into one effective bond. The torsional potentials and the bond-angle potentials that one has to deal with on the atomistic level^[12] are all ignored on the coarse-grained level! All effective beads interact with (truncated and shifted) Lennard-Jones (LJ) potentials,

$$U_{ij} = U_{ij}^{\text{LJ}} + 4\varepsilon S,$$

$$U_{ij}(r \geq r_c = 2\sigma^{7/6}) = 0,$$

$$U_{ij}^{\text{LJ}} = 4\varepsilon \left[\left(\frac{\sigma}{r_{ij}} \right)^{12} - \left(\frac{\sigma}{r_{ij}} \right)^6 \right], \quad (1)$$

where the constant $S (= 127/16384)$ is chosen such that the potential is continuous everywhere. Note that σ denotes the range and ε the strength of this LJ potential. In addition, we use the well-known FENE potential for the bonded beads^[13]

$$U_{\text{FENE}}(r) = -33.75\varepsilon \ln \left[1 - \left(\frac{r}{1.5\sigma} \right)^2 \right]. \quad (2)$$

While in polymer science, considering the fact that a large polymer coil exhibits nontrivial geometric structure on scales from 0.1 nm to 10 nm, and the spectrum of its relaxation times extends over many decades, it is broadly accepted that for most purposes, the use of coarse-grained models is advisable.^[12,14,15] It is less common to also coarse-grain small molecules, such as CO₂ (Figure 1). We represent CO₂ also as a point particle, interacting with LJ potentials, but allow in addition for a quadrupole moment at this molecule (unlike Ref. [14]). Of course, for a simulation of a polymer solution, it would make no sense to coarse-grain only the polymer (Figure 1), but treat the solvent in full atomistic detail. We shall return later to the question how the parameters used for CO₂ have to be determined.

For an alkane chain C_nH_{2n+2}, there are then two parameters ε_n , σ_n to be determined (individually for each choice of n). This is done by requesting that the simulated phase diagram of a pure alkane fluid reproduces precisely the critical temperature $T_c^{(n)}$ and critical density $\rho_c^{(n)}$ of the liquid-vapor transition of this fluid. Grand canonical Monte Carlo methods^[12,14,16,17] in conjunction with histogram extrapolation,^[18] successive umbrella sampling,^[19] and finite size scaling,^[12,14,16,17,20,21] can yield critical temperatures with a relative accuracy of at least 3/1000 and critical densities with a relative accuracy of at least 1/100 with modest effort,^[14,16,22] and hence ε_n , σ_n can be determined with sufficient accuracy.

However ε_n and σ_n are fitted to each substance but follow a smooth trend as a function of chain length and can therefore also be extrapolated for predictive purposes.^[14] Using these parameters, one then can predict from the simulation^[23] the full vapor-liquid coexistence curves in the T - ρ plane (Figure 2), the vapor pressure at coexistence in the T - p plane (Figure 3), and the temperature dependence of the interface tension between the coexisting phases (Figure 4), and compare with experiment.^[11] Note that for each material, only

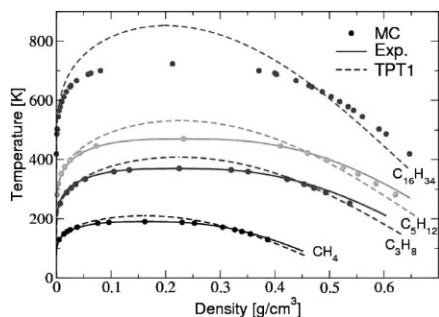


Figure 2.

Coexistence curves for methane (CH_4), propane (C_3H_8), pentane (C_5H_{12}), and hexadecane ($\text{C}_{16}\text{H}_{34}$), from below to above, in the (T - p) plane. Full curves are experimental data,^[1] while the open circles are our simulation results (note that for $\text{C}_{16}\text{H}_{34}$, only data for the critical point but not the whole coexistence curve are available). Broken curves denote estimates from an EOS, obtained via mean field approximations.^[23] Note that both, methane and propane, are modelled as simple effective beads, while pentane is modelled as a dimer, and hexadecane as a pentamer (Figure 1). From.^[23]

two parameters ($T_c^{(n)}$, $\rho_c^{(n)}$) are adjusted via the choice of ε_n , σ_n and three nontrivial curves are predicted; thus the good agreement with experiment is ample evidence that the accuracy of our modeling is sufficiently accurate, despite the drastic approximation inherent in our simple coarse-graining.

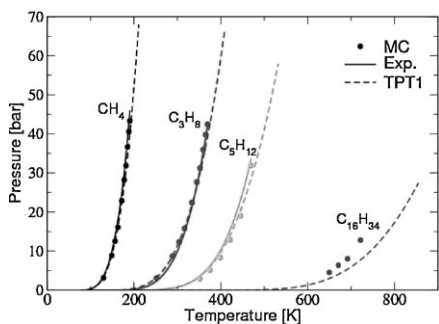


Figure 3.

Coexistence pressures plotted vs. temperature, for the alkanes studied in the present paper, namely CH_4 , C_3H_8 , C_5H_{12} , and $\text{C}_{16}\text{H}_{34}$ (from left to right). Full curves are experimental data,^[1] dots show simulation results, and broken curves are due to an EOS obtained via mean field approximation. From.^[23]

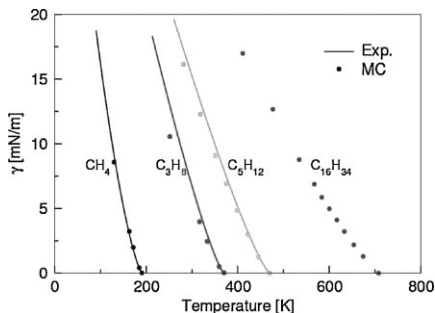


Figure 4.

Interface tensions plotted vs. temperature, for the alkanes studied in the present paper, namely CH_4 , C_3H_8 , C_5H_{12} , and $\text{C}_{16}\text{H}_{34}$ (from left to right). Curves are experimental data,^[1] dots are simulation results. From.^[23]

In Figure 2–3, we have also included an approximate analytic EOS, based on thermodynamic perturbation theory (TPT1 for complex fluids), together with the mean spherical approximation (MSA).^[23–27] This EOS uses the same model, Equation (1) and (2), with the same parameters ε_n , σ_n as the Monte Carlo simulation, but involves a mean field approximation, and therefore the critical temperatures predicted from this EOS are always somewhat too high (and thus, the two-phase coexistence regions too large). Such errors are very common for mean-field type approximations. However, the TPT1-MSA also does not reproduce correctly the liquid branch of the Monte Carlo data for C_5H_{12} and $\text{C}_{16}\text{H}_{34}$, unlike the molecules CH_4 and C_3H_8 that still are modelled as single beads. Similarly, deviations also occur in the vapour pressures at coexistence in the larger molecules, but not in the smaller ones, at low temperatures, between TPT1-MSA and Monte Carlo results. This indicates that TPT1-MSA does not deal with the configurational statistics of short chain molecules correctly. It is clear that, due to all these inaccuracies, any discrepancies between TPT1-MSA results for mixtures, and corresponding experimental data will be delicate to interpret: it then will not be easy to distinguish what discrepancies should be attributed to failures of the TPT1-MSA, and what to failures of the Lorentz-Berthelot

rule. If one would readjust the interaction parameters $\varepsilon_n \sigma_n$ to improve the agreement between TPT1-MSA and experiment, this would introduce other uncontrolled errors. However, the reader should not misunderstand these remarks as a specific criticism of TPT1-MSA; the latter method certainly is one of the best methods to derive an analytic EOS, and our comments are to be understood as a general warning against misinterpretations of discrepancies between any approximate EOS and experiment, taking TPT1-MSA only as an example.

Now, we turn to molecules, such as CO₂ and C₆H₆, which carry a quadrupole moment (but note that CO₂ is a linear molecule while C₆H₆ is disklike). In,^[22] it was shown that a very good description for such molecules is obtained if one augments Equation (1) by a quadrupole-quadrupole interaction term, which is only a relatively small perturbation of the LJ interaction, and this can be treated via thermodynamic perturbation theory. Thus, Equation (1) is replaced by ($U_{ij}(\mathbf{r}_{ij} \geq r_c) = 0$)

$$U_{ij} = 4\varepsilon \left[\left(\frac{\sigma}{r_{ij}} \right)^{12} - \left(\frac{\sigma}{r_{ij}} \right)^6 - \frac{7}{20} q(T) \left(\frac{\sigma}{r_{ij}} \right)^{10} + S \right], \quad (3)$$

where now $S = 127/16384 + (7/5)q(T)/2^{35/3}$ and $q(T)$ is related to the quadrupole moment Q ,

$$q(T) = \frac{Q^4}{\varepsilon \sigma^{10} K_B T} = q_c \frac{T_c}{T}, \quad (4)$$

$$q_c \equiv q(T_c).$$

Using Equation (3), (4), one wishes to fix ε and σ such that again the experimental values for T_c and ρ_c are reproduced. Since ε and σ occur also in $q(T)$, this leads to a self-consistency problem. Defining scaled quantities $T^* = K_B T / \varepsilon$ and $\rho^* = \rho \sigma^3 N_A / M_{mol}$ one requires

$$\varepsilon(q_c) = K_B \frac{T_c}{T_c^*(q_c)}, \quad (5)$$

$$\sigma^3(q_c) = \frac{\rho_c^*(q_c) M_{mol}}{\rho_c N_A},$$

where M_{mol} is the molar mass of the molecule and N_A is Avogadro's number. This self-consistency problem was then solved^[22] by determining the functions $T_c(q_c)/T_c(0)$ and $\rho_c(q_c)/\rho_c(0)$. Using the experimental value $Q = 4.3 \text{ D}\text{\AA}$ in Equation (4) for CO₂ then yields

$$q_c = 0.387, \quad \varepsilon = 3.49110^{-21} \text{ J}, \quad (6)$$

$$\sigma = 3.785 \text{ \AA}.$$

Since Q is only known within some experimental error (which is greatly magnified in q_c , since there Q^4 enters), another plausible choice still consistent with the experimental Q , but better for the description of the vapor-liquid equilibrium data for CO₂, would be

$$q_c = 0.47, \quad \varepsilon = 3.349 \cdot 10^{-21} \text{ J}, \quad (7)$$

$$\sigma = 3.803 \text{ \AA}.$$

Figure 5, 6 show a comparison between our Monte Carlo results based on Equation (6), (7) and experimental data^[11] and five other calculations (discussed in^[22]) all based on rather sophisticated all-atom models of CO₂, plus eventually input from quantum-chemistry calculations. We stress, however, that the problem of solving the many body Schrödinger equation for all electrons and nuclei of two interacting CO₂ molecules is far too complicated, and thus the problem of finding “ab initio” a very accurate effective potential, that could be used in Monte Carlo and Molecular Dynamics work, is still elusive. Thus, one has to be satisfied that without any input about the equation of state, one can predict coexistence curves in the (T, p) and (ρ, T) planes only very roughly.

We comment further that both choices Equation (6), (7) reproduce very nicely also the experimental interfacial tension of CO₂,^[22] and moreover also supercritical isobars are very accurately described (Figure 7).^[28] This figure illustrates two additional points: (i) when one uses the full angle-dependent quadrupolar interaction (rather than reducing it to Equation (3), (4), perturbatively) and recalls the parameters

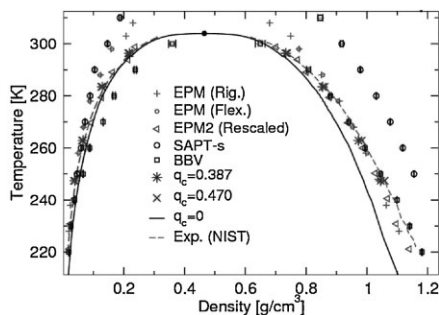


Figure 5.

(Color online) Coexistence curve for CO₂ in the T - ρ plane. Broken curves are the experimental data,^[11] full curve is a simple LJ model (no quadrupole moment). The asterisks (*) and (x) denote the Monte Carlo data using Equation (3), (4) with the choices Equation (6) or (7), respectively. The symbols denoted EPM (Rig.), EPM (Flex.), SAPT-s and BBV show results obtained from “ab-initio” all atoms potentials in simulations (see^[22] for a more detailed discussion and references). The symbols named EPM2 denote data where the EPM potential was rescaled such to reproduce T_c and ρ_c as well. From.^[22]

such that again the experimental T_c , ρ_c are reproduced, the results are almost indistinguishable. (ii) When one uses ϵ , σ , and q_c as an input into a classical density functional calculation, the results are in very good agreement with both experiment and Monte Carlo simulation.^[28] Note, however, that the density functional method (see^[28] for a description and references) cannot be applied very close to the critical point.

Finally, we note that Equation (3), (4) yield very good results also for other

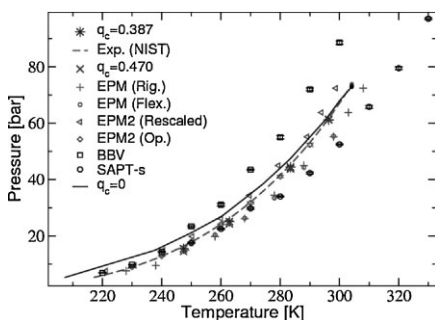


Figure 6.

(Color online) Same as Figure 5, but for the vapor pressure at coexistence. Note that the rescaled EPM2 data do not reproduce the experiment well. From.^[22]

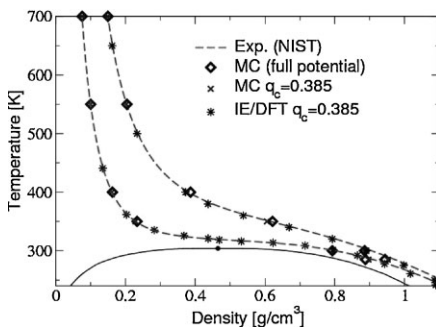


Figure 7.

(Color online) Supercritical isobars at $p=200$ bar (topmost curve^[11]) and $p=100$ bar (middle curve^[11]) in the T - ρ plane. Full curve is the coexistence curve. Diamonds show Monte Carlo data using the full quadrupolar interactions,^[28] asterisks density functional results (see^[28] and references therein). From.^[28]

quadrupolar fluids, such as benzene.^[22] Of course, if one goes very far below the critical point (i.e., $T=0.6T_c$ or less), slight deviations between model predictions and experiment become noticeable. This must be expected, of course; the denser the liquid, the more problematic the coarse-graining becomes, and in the solid phases of molecular fluids, such as short alkanes, CO₂, C₆H₆ etc., it cannot work at all. But we maintain that the approach is rather accurate and useful for a broad range of temperatures and pressures.

Mixtures and Solutions

When one wishes to treat a binary system (A, B), extending our model description in terms of LJ interactions between the particles, an assumption on the interactions between unlike particles needs to be made. We here use the Lorentz-Berthelot mixing rule^[10]

$$\sigma_{AB} = (\sigma_{AA} + \sigma_{BB})/2, \quad (8)$$

$$\epsilon_{AB} = \sqrt{\epsilon_{AA} \epsilon_{BB}}$$

We test this rule by computing isothermal slices through selected binary (T_c , p , x) phase diagrams, where experimental data are available, for mixtures of systems that

have been described in Sec. II. Since the parameters ϵ_{AA} , σ_{AA} , ϵ_{BB} , σ_{BB} have already been fixed (Sec. II), no more adjustable parameters whatsoever are available.

The simplest case is a mixture of methane and propane: both molecules are modelled as simple beads, and no quadrupolar interactions are involved. Figure 8 shows two examples, where we compare data^[29] to our Monte Carlo results and TPT1-MSA calculations.^[23]

One can see that near the ordinate axis (pure Propane) at the higher temperature, there is almost perfect agreement between TPT1-MSA, experiment and simulation, while the data deviate somewhat near the critical point: the simulation predicts a somewhat too small two-phase region, while TPT1-MSA predicts a much too large loop (because of its mean field character, too large loops are expected). At the lower temperature, $T = 277$ K, the relative deviations between the calculated and observed loops are somewhat smaller, but deviations start out at small x already (the slope of the vapour pressure vs- x curve is slightly incorrect). Note, however, that at this temperature, we are already relatively far below the critical temperature of pure C_3H_8 .

Similar good agreement between experiment, simulation and TPT1-MSA (that includes the averaged quadrupolar interaction) is noted when one considers

the $CH_4 + CO_2$ system (Figure 9a), apart from the usual problem that the TPT1-MSA overestimates the size of the two-phase coexistence region near criticality. Neglecting the quadrupole moment, however, leads to the more pronounced systematic deviations. Similar conclusions hold for the $CO_2 + C_5H_{12}$ system, although there, the gas branch prediction of TPT1-MSA has more pronounced systematic deviations from both experiment and simulation than the $CO_2 + CH_4$ system.

Now, we finally return to the $CO_2 + C_{16}H_{34}$ system (Figure 10, 11). These data clearly show that the model for CO_2 with q_c in the range from $q_c = 0.387$ to $q_c = 0.47$ leads to roughly the same results as a model with no quadrupole moment, but strongly violating the Lorentz-Berthelot rule, $\epsilon_{AB} = \xi(\epsilon_{AA}\epsilon_{BB})^{0.5}$ with $\xi = 0.9$. Since it was shown^[14] that a satisfactory agreement between experiment for the $CO_2 + C_{16}H_{34}$ system is obtained if one uses a pure LJ model for CO_2 , but allows for a strong violation of the Lorentz-Berthelot rule, taking $\xi \approx 0.886$, we see that most of this strong violation of the Lorentz-Berthelot mixing rule simply comes from an inadequate modelling of CO_2 . We estimate that the present model, based on Equation (3–7), would fit the experimental data almost precisely, if a deviation of ξ from unity by 1–2% would be admitted. Such small deviations from the Lorentz-Berthelot

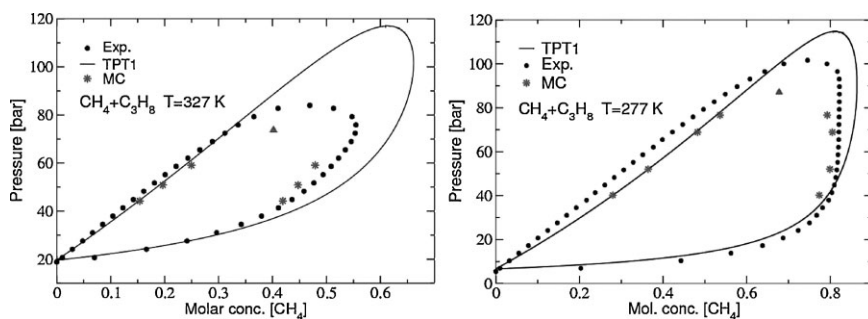


Figure 8.

(Color online) Isothermal slice through the phase diagram of the mixture of CH_4 and C_3H_8 , $T = 327$ K (a) and $T = 277$ K (b), using the molar fraction x of CH_4 , as abscissa variable and pressure p as the ordinate variable. Dots (black) are the experimental data,^[29] the curve denotes the TPT1-MSA approximation, asterisks (red) and triangles (the latter show the locations of the critical points) are the Monte Carlo results. From.^[23]

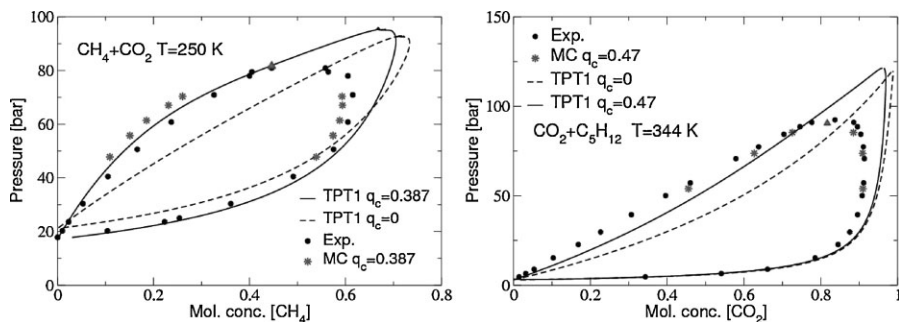


Figure 9.

(Color online) Isothermal slices through the phase diagrams of the mixture of CH₄+CO₂ at $T = 250$ K (a) and the mixture of CO₂+C₅H₁₂ at $T = 344$ K (b). Dots represent experimental results,^[29,30] asterisks denote Monte Carlo results, triangles critical point estimates from the Monte Carlo calculation, while full and broken curves show the TPT1-MSA results for the polar model ($q_c > 0$) and the apolar one ($q_c = 0$), respectively. From.^[23]

mixing rules are entirely expected. There is little reason to believe that the mixing rule is exact. We feel, however, that the present level of modelling based strictly on Equation (8) but including quadrupolar interactions via Equation (3–7), whenever appropriate, leads to a fairly accurate description, with small enough errors so that this type of modelling still is useful.

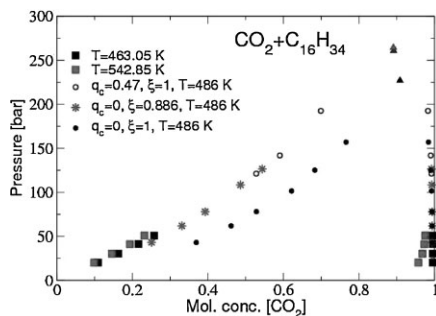


Figure 10.

(Color online) Isothermal slice through the phase diagram of the CO₂+C₁₆H₃₄ system, at $T = 486$ K, showing Monte Carlo results for the present model (open circles) and results for a model where CO₂ was described by a LJ particle with no quadrupole moment (full dots)^[14] and a variant for this model, where $\epsilon_{AB} = (\epsilon_{AA}\epsilon_{BB})^{0.5}$ was taken, with $\xi = 0.886$.^[14] Squares show two sets of experimental data^[31] at two temperatures that bracket the temperature used in the simulation. Triangles are Monte Carlo results for the critical point. From.^[23]

In conclusion, to the question “can one predict the phase behavior of simple fluids, fluid mixtures, and polymer solutions”, the answer is “yes and no”: one does need some experimental input (critical temperatures and densities of the pure components were used here, as well as reasonable estimates for the quadrupole moment of the solvent molecules, if they have one). Then, one can make rather reliable predictions; the accuracy of these predictions is still not perfect, but it is rather good.

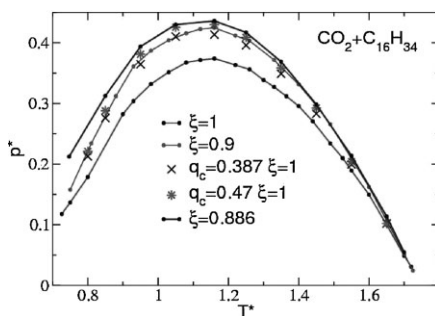


Figure 11.

(Color online) Critical curve of the CO₂+C₁₆H₃₄ mixture, projected onto the (p^* , T^*) plane ($p = p^*/\sigma^3$, $T = T^*/\epsilon/K_B$), using LJ parameters of hexadecane. Different symbols (as indicated in the figure) denote data with $q_c = 0$, $\xi = 0.886$ (top curve), and $\xi = 0.9$, $\xi = 1$ (lowest curve), as well as the data for nonzero quadrupole moment, $q_c = 0.387$ and $q_c = 0.47$, respectively. From.^[23]

Acknowledgements: This research was supported in part by BASF SE (Ludwigshafen) and the Deutsche Forschungsgemeinschaft (DFG).

- [1] P. J. Flory, *J. Chem. Phys.* **1941**, 9, 660; M. L. Huggins, *J. Chem. Phys.* **1941**, 9, 440.
- [2] P. J. Flory, *Principles of Polymer Chemistry*, Cornell Univ. Press, Ithaca **1953**.
- [3] *Supercritical Fluids*, E., Kiran, J. M. H. Levelt-Sengers, Eds., Kluwer Acad. Publ, Dordrecht **1994**.
- [4] *Supercritical Carbon Dioxide in Polymer Reaction*, M. Kemmere., Th. Meyer, Eds., Wiley-VCH, Weinheim **2005**.
- [5] B. Krause, H. J. P. Sijbesma, P. Münöklü, N. F. A. van der Vegt, M. Wessling, *Macromolecules* **2001**, 34, 8792.
- [6] J. S. Rowlinson, F. L. Swinton, *Liquids and Liquid Mixtures*, Butterworths, London **1982**.
- [7] R. L. Scott, P. H. von Konynenburg, *Discuss. Faraday Soc.* **1970**, 49, 87; P. H. von Konynenburg, R. L. Scott, *Phil. Trans. R. Soc. London Ser. A* **1980**, 298, 495.
- [8] G. Schneider, Z. Alwani, W. Heim, E. Horvath, E. U. Franck, *Chemie-Ing. Tech.* **1967**, 39, 649.
- [9] J. D. Hottovy, K. D. Luks, J. P. Kohn, *Chem. Eng. Data* **1981**, 26, 256.
- [10] G. C. Maitland, M. Rigby, E. B. Smith, W. A. Wakeham, *Intermolecular Forces, Their Origin and Determination*, Clarendon Press, Oxford **1981**.
- [11] NIST website: <http://webbook.nist.gov/chemistry/>.
- [12] K. Binder in, *Monte Carlo and Molecular Dynamics Simulations in Polymer Science*, Oxford Univ. Press, New York **1995**.
- [13] K. Kremer, G. Grest, *J. Chem. Phys.* **1990**, 92, 5057.
- [14] K. Binder, M. Müller, P. Virnau, L. G. MacDowell, *Adv. Polym. Sci.* **2005**, 173, 1.
- [15] *Coarse-graining of Condensed-Phase and Biomolecular Systems*, G. Voth, Eds., Taylor & Francis, in press.
- [16] N. B. Wilding, *J. Phys. : Condensed Matter* **1997**, 9, 585.
- [17] D. P. Landau, K. Binder, *A Guide to Monte Carlo Simulations in Statistical Physics*, 2nd ed., Cambridge Univ. Press, Cambridge **2005**.
- [18] A. M. Ferrenberg, R. H. Swendsen, *Phys. Rev. Lett.* **1988**, 61, 2635; *ibid* **1989**, 63, 1195.
- [19] P. Virnau, M. Müller, *J. Chem. Phys.* **2004**, 120, 10925.
- [20] M. E. Fisher, in *Critical Phenomena*, Academic Press, London **1971**.
- [21] K. Binder, *Z. Physik B* **1981**, 43, 119.
- [22] B. M. Mognetti, L. Yelash, P. Virnau, W. Paul, K. Binder, M. Müller, L. G. MacDowell, *J. Chem. Phys.* **2008**, 128, 104501.
- [23] B. M. Mognetti, P. Virnau, L. Yelash, W. Paul, K. Binder, M. Müller, L. G. MacDowell, *To be published*.
- [24] M. S. Wertheim, *J. Chem. Phys.* **1987**, 87, 7323.
- [25] Y. Tang, B. C.-Y. Lu, *J. Chem. Phys.* **1993**, 99, 9828.
- [26] Y. Tang, Z. Tong, B. C.-Y. Lu, *Fluid Phase Equilib.* **1997**, 134, 21.
- [27] L. G. MacDowell, M. Müller, C. Vega, K. Binder, *J. Chem. Phys.* **2000**, 113, 419.
- [28] B. M. Mognetti, M. Oettel, L. Yelash, P. Virnau, W. Paul, K. Binder, *Phys. Rev. E* **2008**, 77, 041506.
- [29] B. H. Sage, W. N. Lacey, J. G. Schaafsma, *Ind. Eng. Chem.* **1934**, 26, 214.
- [30] H. Cheng, M. E. P. de Fernandez, J. A. Zollweg, W. B. Streett, *J. Chem. Eng. Data* **1989**, 34, 319.
- [31] H. M. Sebastian, J. J. Simnick, H.-M. Liu, K.-C. Chao, *J. Chem. Eng. Data* **1980**, 25, 138.